Available online at www.sciencedirect.com
ScienceDirect
International Journal of Pharmaceutics 334 (2007) 156–165
INTERNATIONAL JOURNAL OF PHARMACEUTICS
www.elsevier.com/locate/ijpharm

Pharmaceutical Nanotechnology

Evaluation of bioadhesive potential and intestinal transport of pegylated poly(anhydride) nanoparticles

K. Yoncheva [a,d], L. Guembe [b], M.A. Campanero [c], J.M. Irache [a,*]

[a] *Centro Galénico, University of Navarra, Apartado 177, 31080 Pamplona, Spain*
[b] *Morphology and Image Unit, School of Medicine, Centre for Applied Medical Research (CIMA), University of Navarra, 31080 Pamplona, Spain*
[c] *Servicio de Farmacología Clínica, CUN, University of Navarra, Pamplona, Spain*
[d] *Department of Pharmaceutical Technology, Faculty of Pharmacy, 2 Dunav Str., 1000 Sofia, Bulgaria*

Received 22 May 2006; received in revised form 7 October 2006; accepted 9 October 2006
Available online 13 October 2006

Abstract

Nanoparticles based on the poly(methyl vinyl ether-*co*-maleic anhydride) were pegylated with different types of PEGs, namely, two hydroxyl-functionalized PEGs (PEG and mPEG) and two amino-PEGs (DAE-PEG and DAP-PEG). The resulted nanoparticles demonstrated reduction of the negative surface charge compared to the non-modified particles. Further, in vivo experiments showed that all types of pegylated particles possessed higher affinity to adhere to intestinal rather than to the stomach mucosa. Higher bioadhesive potential was observed in the case of PEG-NP and DAE-PEG-NP which was attributed to the flexibility and specific properties of the surface "brush" layer of these particles. The lower bioadhesive potential of mPEG-NP was due to the low presence of coating "brush" layer, whereas for DAP-PEG-NP to the fact that the double end coupled chains ("loop"-conformation) were not available for intensive interactions with the mucosa. The observations made by optic microscopy illustrated an intracellular transport of PEG-NP in vivo with preferable location in the apical area of enterocytes.

Keywords: Nanoparticles; Pegylation; Bioadhesion; Oral administration; Intracellular transport

1. Introduction

Particulate systems have been widely investigated in order to improve the oral availability of numerous drugs (Kreuter, 1991). The main drawback of the oral administration of colloidal particulate systems is their rapid gastrointestinal elimination. For this purpose, bioadhesive polymers could be applied either as particle carriers or as coating agents aiming to overcome the rapid elimination (Sakuma et al., 1999; Kawashima et al., 2000; Vila et al., 2002). Except prolongation of nanoparticle residence time some types of bioadhesive polymers may establish specific interactions with the gastrointestinal mucosa allowing opportunity for target drug delivery (Irache et al., 1996; Hussain et al., 1997) Numerous of drug molecules (particularly macromolecular drugs) presenting low oral bioavailability as well as low stability in the tract could be incorporated in such systems.

In this context, the coating of insulin-loaded liposomes with chitosan, a wide investigated polysaccharide with bioadhesive properties, was considered to be an adequate strategy to reduce the blood glucose levels in rats for at least 12 h after oral administration (Takeuchi et al., 1996).

Polyethylene glycols (PEGs) are hydrophilic, nonionic and non-toxic polymers which are not known like strong bioadhesives compared with chitosan or carbomers. However, few studies have noted the capacity of PEGs to modulate the bioadhesive properties of some delivery systems (De Ascentiis et al., 1995; Huang et al., 2000). Huang et al. (2000) have reported that PEG-chains may establish specific bioadhesive interactions with mucosal tissues because of their ability to interdiffuse across the mucus network. Another interesting data are associated with the ability of PEG-coating layer to enable nanoparticle transport through mucosal barriers. Recently, it has been found that PEG-coated PLGA nanoparticles were more efficient than chitosan-coated particles in facilitating the transport of the associated antigen (tetanus toxoid) through nasal mucosa

* Corresponding autor at: Centro Galénico, Farmacia y Tecnología Farmacéutica, University of Navarra, Apartado. 177, 31080 Pamplona, Spain. Tel.: +34 948 42 5600x6313; fax: +34 948 425649.
E-mail address: jmirache@unav.es (J.M. Irache).

0378-5173/$ – see front matter © 2006 Elsevier B.V. All rights reserved.
doi:10.1016/j.ijpharm.2006.10.016

(Vila et al., 2002). Regarding intestinal transport, the capacity of pegylated nanoparticles to pass through intestinal mucosa was pointed out although the mechanism was not detailed (Tobio et al., 2000). It is generally accepted that nanoparticle uptake could occur via endocytosis by enterocytes (intracellular route), paracellular route or transcytosis via cells of the gut-associated lymphoid tissue (GALT) (Hodges et al., 1995; Florence, 1997). However, how the uptake of pegylated nanoparticles occurred is not well known. Another option of the oral application of pegylated nanoparticles can be an improvement of drug/nanoparticle stability due to the protective properties of PEG-coating layer around nanoparticles (Tobio et al., 2000; Iwanaga et al., 1997). PEG-chains coupled to or physically adsorbed on the surface of nanoparticles exhibit great flexibility in an aqueous medium and have a large excluded volume. The steric repulsion resulting from a loss of conformational entropy of the bound PEG chains upon the approach of a foreign substance and the low interfacial free energy of PEG in water contribute to the extraordinary physiological properties of nanoparticles covered with PEG (Peracchia et al., 1997; Otsuka et al., 2003). This fact is very important taking into account that many of the nanoparticle carriers suffer from rapid degradation under the enzyme activity into the gastrointestinal tract (Ropert et al., 1993; Le Ray et al., 1994). Encouraging, Tobio et al. (2000) have postulated that one of the reasons for the improvement of tetanus toxoid transport across intestinal mucosa was the stabilizing effect of PEG-coating around the nanoparticles developed. Consequently, the development of pegylated nanoparticles could be a promising strategy to design nanoparticles with high stability against gastric enzymes as well as able to develop specific bioadhesive interactions with the intestinal mucosa.

In a previous study we demonstrated the possibility to prepare pegylated nanoparticles based on poly(methyl vinyl ether-*co*-maleic anhydride) under mild conditions (Yoncheva et al., 2005a). The results showed that more efficient pegylation could be achieved using PEG with molecular weight of 2000 Da. Further, the pegylation of polyanhydride nanoparticles was developed because of opportunity to obtain surface-modified nanoparticles with bioadhesive properties different in comparison with the naked nanoparticles. In the present study, PEGs possessing different functional groups (hydroxyl or amino) were used as pegylation agents aiming to investigate their ability as bioadhesive promoters. Another objective of the work was to follow the mode of the transport of developed pegylated nanoparticles across intestinal mucosa.

2. Materials and methods

2.1. Materials

Poly(ethylene glycol) 2000, monomethyl ether of PEG 2000 (mPEG), *O*,*O*′-bis-(2-aminoethyl)polyethylen glycol 2000 (DAE-PEG) and *O*,*O*′-bis-(2-aminopropyl)-polypropilenglycol-polyethylenglycol-polypropilenglycol 2000 (DAP-PEG) were supplied by Fluka (Switzerland). Poly(methyl vinyl ether-*co*-maleic anhydride) (PVM/MA) (Gantrez AN 119; M_w of 200 kDa) was a gift from ISP (Barcelona, Spain). Rhodamine B isothiocyanate (RBITC) and fluorescein isothiocyanate (FITC) were purchased by Sigma (St Louis, USA).

2.2. Preparation of pegylated PVM/MA-nanoparticle

The nanoparticles were prepared using the method previously established for pegylation of PVM/MA nanoparticles (Yoncheva et al., 2005a). Thus, 100 mg of PVM/MA copolymer and 25 mg of PEG were dissolved and stirred in acetone (5 ml) for 1 h. After their incubation, 10 ml of a hydroalcoholic mixture (1:1, v/v) was added to the organic phase. The solvents were eliminated under reduced pressure (Buchi R-144, Switzerland) and nanoparticles were fluorescently labelled either with RBITC (1250 μg) or with FITC (1250 μg) by incubation of the aqueous nanosuspensions with the selected marker for 5 min. The nanoparticles were purified by twice centrifugation at 17,000 rpm for 20 min (Sigma 3K30, Germany) and finally lyophilized (Genesis 12EL, Virtis, USA) using sucrose as cryoprotector (5%, w/v).

Conventional PVM/MA-nanoparticles (NP) were prepared parallely applying the same protocol but in the absence of PEG.

2.3. Characterisation of the pegylated nanoparticles

The nanoparticle size and zeta-potential were determined by photon correlation spectroscopy and electrophoretic laser doppler anemometry using a Zetamaster analyzer (Malvern Instruments, UK). Samples were diluted with 0.05 M phosphate buffered saline (pH 7.4) and measured at 25 °C with a scattering angle of 90°. The shape and surface of resulted particles were observed by transmission electron microscopy (Zeiss-electron microscope) after negative staining of the samples with phosphotungstic acid.

The amounts of PEGs associated to the nanoparticles were determined by nuclear magnetic resonance method (^{1}H NMR) (Brucer Avance 400, Germany) as described previously (Yoncheva et al., 2005a). Thus, exactly weighted amounts of the pegylated nanoparticles (5 mg) were dissolved in deuterated DMSO (0.5 ml) and the spectra were obtained at $n_s = 6400$ or 12,800 (for DAE-PEG-NP and DAP-PEG-NP). ^{1}H NMR spectra of free PEGs were performed using the same ratio and experimental conditions. The quantity of PEG-attached to the nanoparticles was calculated by the ratio between peak areas of the protons of ethylene units (3.51 ppm) detected in the spectra of pegylated particles and in the spectra of free PEGs, respectively.

The amounts of RBITC or FITC loaded to nanoparticles were determined by colorimetry at wavelength 540 or 450 nm, respectively (Labsystems iEMS Reader MF, Finland). The marker loading was calculated after total hydrolysis of a certain amount of nanoparticles in 0.1 N NaOH and expressed in μg/mg nanoparticles.

In vitro release of FITC was studied by dispersing of nanoparticles (6 mg/ml) in both simulated gastric and intestinal fluids (USP XXIII) at 37 °C. At predetermined time intervals, the nanosuspensions were centrifuged (17,000 rpm, 20 min.) and the FITC released was measured in the supernatants by colorimetry ($\lambda = 450$ nm).

2.4. In vivo bioadhesive study

The study was performed in compliance with the regulations of the responsible committee of the University of Navarra in line with the European legislation on animal experiments (86/609/EU). Pegylated nanoparticles loaded with RBITC were administered in the form of aqueous suspensions (10 mg/ml) to fasted Wistar rats perorally. The animals were sacrificed by cervical dislocation at 0.5, 1, 3 and 8 h post-administration. The abdominal cavity was opened and GIT was removed and divided into three regions: stomach, small intestine and caecum. Each segment was opened lengthwise along the mesentery and rinsed with phosphate saline buffer (pH 7.4). Further, each segment was cut into portions of 2 cm length and digested in 1 ml of 3 N NaOH for 24 h (Arbos et al., 2002). RBITC was extracted with 2 ml methanol, vortexed for 1 min and centrifuged at 4000 rpm for 10 min. Aliquots (1 ml) of the supernatants were assayed for RBITC by spectrofluorimetry (GENios, Austria) to estimate the fraction of adhered nanoparticles to the mucosa.

Control RBITC solution (100 μg/ml) was administered to rats and RBITC fractions within gastrointestinal mucosa were determined following the same procedures as above.

2.5. Bioadhesive parameters

The total adhered fractions of the pegylated nanoparticles in the whole gastrointestinal tract were plotted versus time and the parameters of bioadhesion (Q_{max}, AUC_{adh}, k_{adh} and MRT_{adh}) were estimated as described previously (Arbos et al., 2002, 2003). Q_{max} is the maximal amount of nanoparticles adhered to the gut surface and is related with the capability of nanoparticles to develop adhesive interactions. k_{adh} was defined as the terminal elimination rate of the adhered fraction with the gastrointestinal mucosa. AUC_{adh} or the area under the curve of bioadhesion was evaluated by means of the trapezoidal rule up to t_z, which denoted the last sampling point, and permitted to quantify the intensity of the bioadhesive phenomenon. Finally, MRT_{adh} was the mean residence time of the adhered fraction of nanoparticles in the mucosa and evaluated the relative duration of the adhesive interactions. All of these parameters were estimated from 0 to 8 h and calculated according to the resulted curves using WinNonlin 1.5 software (Pharsight Corporation, USA).

2.6. Morphological studies

Pegylated nanoparticles loaded with FITC as well as control solutions of FITC (45 and 150 μg/ml) were administered perorally to fasted rats and the animals were sacrificed one hour post-administration. Segments of the jejunal and ileal parts of the small intestine were taken, rinsed with a phosphate buffer and immersed in a formalin medium (4%) for 24 h. After fixation, the tissues samples were paraffin embedded, cut into sections with a thickness of 3 μm and mounted on slides coated with Vectabond (Vector Laboratories, Burlingame, CA, USA). Further, tissue sections were deparaffinized, rehydrated and the endogenous peroxidase was blocked by addition of H_2O_2 (3%) for 10 min. Thereafter, the slides were treated as follow: washed with distilled water for 5 min, placed in a citrate buffer (0.01 M, pH 6.0) and heated in a microwave two times for 15 min (at maximal and minimal power), washed with tap water and finally with a Tris buffer (0.05 M, pH 7.36). To avoid non-specific staining, sections were incubated with a normal goat serum (1:20, DAKO, Carpinteria, CA, USA) at room temperature for 30 min and after that with specific antiserum (monoclonal anti-FITC, M0878, DAKO, CA, USA). The latter was added to the sections in different dilutions (1:100, 1:400, 1:1000 and 1:1500) and incubated at 4 °C overnight. Immunocytochemical staining for FITC was performed using the Envision™ + System (DAKO, Carpinteria, CA, USA). After rinsing with TBS, the sections were incubated with the secondary antibody, goat anti-mouse Ig coupled to a peroxidase-labeled dextran at room temperature for 30 min. The sections were then rinsed with TBS and the peroxidase activity was revealed in a working solution containing diaminobenzidine as a chromogen. Paralelly, negative controls were made by omission of the primary antibody. The sections were lightly counterstained with a haematoxylin, dehydrated and mounted in DPX. The sections were observed by optical microscope (Nikon Eclipse E 800M, Japan) equipped with a digital camera (Nikon DXM 1200).

2.7. Statistical studies

The bioadhesion data and the physicochemical characteristics were compared using the nonparametric Mann–Whitney *U*-test and Student *t*-test, respectively. *P* values of <0.05 were considered significant. All calculations were performed using SPSS® statistical software program (SPSS® 10, Microsoft, USA).

3. Results and discussion

In the present study the bioadhesive potential of pegylated nanoparticles was examined. For this purpose, four different PEGs, possessing equal molecular weight but different functional groups, were used as pegylation agents. Conventional PEG with two hydroxyl groups, methoxy-PEG and two amino-functionalized PEGs with different properties were selected for the study.

3.1. Characterization of the nanoparticles

The first step for the preparation of pegylated nanoparticles was the simultaneous incubation between PEG and PVM/MA copolymer in acetone. This incubation would promote the reaction between hydroxyl or/and amino groups of PEG molecules with the anhydride residues of PVM/MA. Then, nanoparticles were obtained by a solvent-displacement method and non-associated fractions of PEG and PVM/MA were easily removed during the purification step by centrifugation.

As it can be seen, higher pegylation degree was achieved using amino-functionalized PEGs (DAE-PEG 2000 and DAP-PEG 2000) compared to hydroxy-functionalized PEGs (PEG 2000 and mPEG 2000) (Table 1). This fact was attributed to the higher affinity of acid anhydride residues of PVM/MA to amino groups (Schmidt et al., 2003; Pompe et al., 2003). Thus, the pegy-

Table 1
Physicochemical properties of the pegylated nanoparticles

Sample	Size (nm)	Zeta-potential (mV)	Associated PEG (μg/mg)[a]	RBITC loaded (μg/mg)[b]
NP	289 ± 11	−58.8 ± 4.5	–	10.33 ± 0.87
PEG-NP	299 ± 22	−44.1 ± 5.2*	30.2 ± 4.0	10.37 ± 0.09
mPEG-NP	272 ± 17	−48.6 ± 0.5*	36.6 ± 2.9	10.46 ± 0.11
DAE-PEG-NP	505 ± 88*	−30.1 ± 0.5*	76.5 ± 1.5	10.04 ± 0.62
DAP-PEG-NP	361 ± 15*	−11.5 ± 0.1*	82.9 ± 2.2	8.74 ± 0.75*

Data express mean ± S.D. ($n = 6$).
[a] Amount of PEG bound to the nanoparticles (μg/mg) determined by ^{1}H NMR spectroscopy.
[b] Quantity of RBITC loaded to the nanoparticles (μg/mg) measured by colorimetry.
* $P < 0.05$; pegylated nanoparticles versus control nanoparticles (NP) (Student t-test).

lation probably occurred by formation of amide bonds between anhydride residues of PVM/MA and amino groups of PEGs. The latter was in accordance with another study where formation of amide bonds between anhydride groups of PVM/MA and amino groups of various proteins has been demonstrated (Isosaki et al., 1992).

The main physicochemical characteristics of the resulted pegylated nanoparticles are summarised in Table 1. Regarding zeta potential, all modified nanoparticles demonstrated reduction of the negative surface charge compared to the conventional PVM/MA-particles ($p < 0.05$). However, some differences were observed depending on the pegylating agent used, and, as a consequence, the different way of their association to PVM/MA during nanoparticle formation. The lower negative value for PEG-NP was attributed to the presence of PEG "brush" layer around these particles as it was previously corroborated by ^{1}H NMR spectroscopy (Yoncheva et al., 2005a). The same method was performed in order to determine the conformation state of PEG-chains after binding to the other types of particles developed here. Thus, comparative ratio between the peak area of protons of ethylene groups (3.51 ppm) and protons of OH- or NH_2-groups for both free PEGs (as control) and pegylated nanoparticles was formulated. The values of the ratio for nanoparticle samples and free PEGs are summarized in Table 2. Regarding m-PEG-NP, the calculations showed slightly higher ratio between ethylene protons and hydroxyl protons for mPEG-NP than for free mPEG due to the reduction of the area of available hydroxyl protons. This fact suggested that only a reduced amount of the OH-residues of mPEG was able to react with the anhydride groups of PVM/MA during nanoparticle formation. Since the predominant part of hydroxyl protons kept their conformation it could be considered that the larger number of OH-groups did not participate in any coupling reaction. Hence, three possibilities could be considered: physical adsorption of the mPEG chains on the nanoparticle surface, distribution of mPEG into the matrix of the resulting nanoparticles or reaction of a small fraction of mPEG extended in a "brush" conformation (Fig. 1B). From these three possibilities, the physical adsorption of the mPEG chains on the nanoparticle surface appeared to be the most probable. In fact, the moderate reduction of zeta potential observed for mPEG-NP, compared with that of control nanoparticles (Table 1), appeared to support this possibility.

Fig. 2 shows the ^{1}H NMR spectra of free DAP-PEG and the nanoparticles pegylated with this agent. As it can be seen, the protons of both amino groups (4.58 and 4.45 ppm) of DAP-PEG did not appear in the spectra of DAP-PEG-NP which led to the assumption that all amino-groups were coupled to the anhydride residues of PVM/MA. This fact suggested that the chains of this PEG derivative were bound to the surface of nanoparticles by both functionalized ends forming a "loop" conformation (Fig. 1D). In this view, TEM photographs revealed that these particles were surrounded by a thin but continuous layer (Fig. 3A),

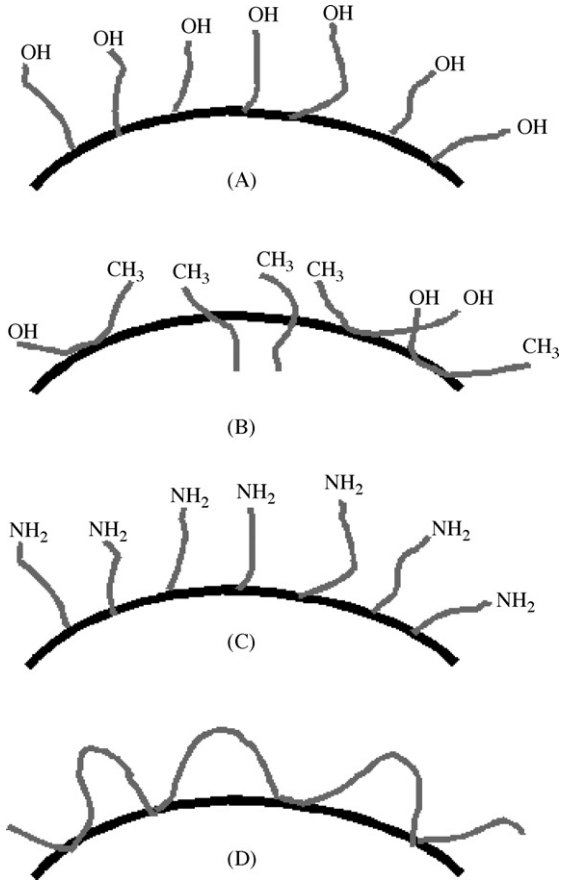

Fig. 1. Hypothesized configuration of PEG chains at the surface of nanoparticles prepared with PEG (A), mPEG (B), DAE-PEG (C), or DAP-PEG (D). PEG chains: grey lines.

Table 2
Quantitative data obtained by ^{1}H NMR-spectra of the pegylated nanoparticles and free PEGs as controls

Sample	Peak A (ethylene protons) 3.51 ppm	Peak B hydroxyl/amino protons 4.58 ppm	Peak C amino protons 4.45 ppm	Ratio A/B
PEG	753.5×10^8	7.36×10^8	–	102.4
PEG-NP	20.3×10^8	0.11×10^8	–	184.5
mPEG	460.0×10^8	2.601×10^8	–	176.8
mPEG-NP	23.0×10^8	0.106×10^8	–	217.0
DAE-PEG[a]	286.5×10^8	ND	ND	–
DAE-PEG-NP[a]	21.7×10^8	ND	ND	–
DAP-PEG[a]	1151.4×10^8	0.098×10^8	0.215×10^8	–
DAP-PEG-NP[a]	98.06×10^8	ND	ND	–

Peak A corresponded to protons of ethylene units (–OCH_2CH_2–, $\delta = 3.51$ ppm); peak B to protons of hydroxyl/amino groups of PEGs ($\delta = 4.58$ ppm); peak C to protons of amino groups ($\delta = 4.45$ ppm).
[a] ^{1}H NMR spectra of both free amino-PEGs and amino-pegylated nanoparticles were performed at $n_s = 12{,}800$.

whereas, for comparison, PEG-NP were surrounded by a fluffy coat presumably consisting of PEG-chains in a "brush" conformation (Fig. 3B).

Finally, for DAE-PEG-NP, the signal of amino-protons always appeared (not shown), but, because of its weak intensity (in the form of plateau) the quantitative ratio was not possible to establish. However, the appearance of the amino-protons in the spectrum denoted that "loop" conformation was not formed. In this case, the only logical explanation is that the chains of DAE-PEG were spread from the nanoparticle surface in a "brush" conformation rather than forming a "loop" type disposition (Fig. 1C).

3.2. Bioadhesive properties of the nanoparticles

In vivo bioadhesive studies were performed using pegylated nanoparticles loaded with RBITC. To ensure that the fluorescence determined in the gastrointestinal parts was due to

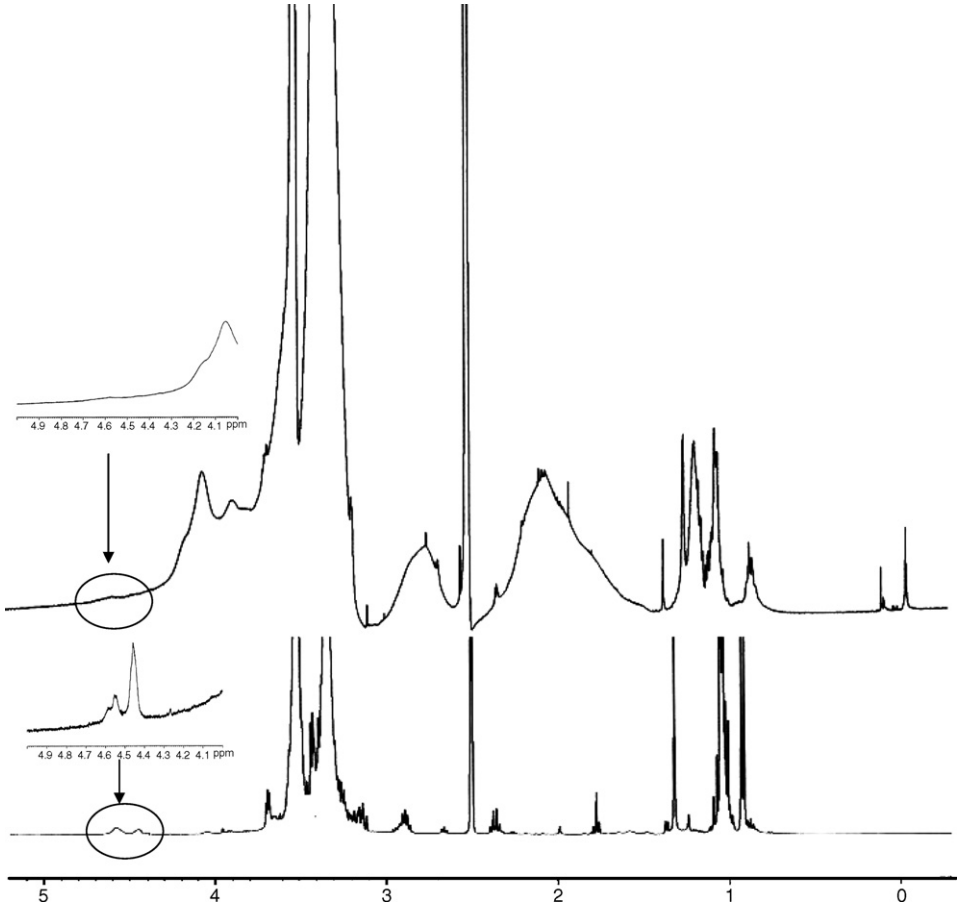

Fig. 2. ^{1}H NMR spectra of free DAP-PEG (bottom) and DAP-PEG-NP (top) performed in DMSO at $n_s = 12{,}800$. In the small figures: increased image of both peaks of the amino-protons of DAP-PEG (bottom) and its absence in the spectrum of DAP-PEG-NP (top).

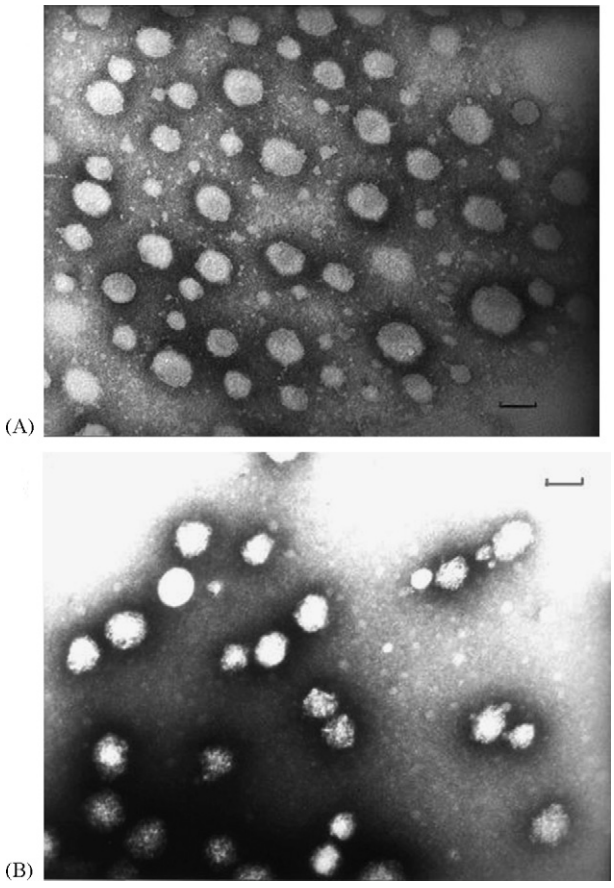

Fig. 3. Transmission electron microscopy of (A) DAP-PEG-NP and (B) PEG-NP. Bar represents 150 nm.

the RBITC-associated nanoparticles, control RBITC-solution was administered to rats. The results showed that three hours after oral administration approximately 5% of RBITC was spread on the whole GIT versus 16–25% adhered fractions for pegylated nanoparticles (Fig. 4). In addition, RBITC was not found 8 h after administration of RBITC-solution (data not shown) whereas 6–12% of nanoparticles were still adhered to the mucosa. The data also showed that the bioadhesive maximum of non-pegylated NP appeared half of hour after their oral administration and decreased very rapidly with the time. On the contrary, pegylated particles demonstrated lower initial capacity to develop bioadhesive interactions although it was maintained for at least 3 h. The quantity of the adhered fractions varied from 25% of the administered dose for PEG-NP to 16% for DAP-PEG-NP, respectively.

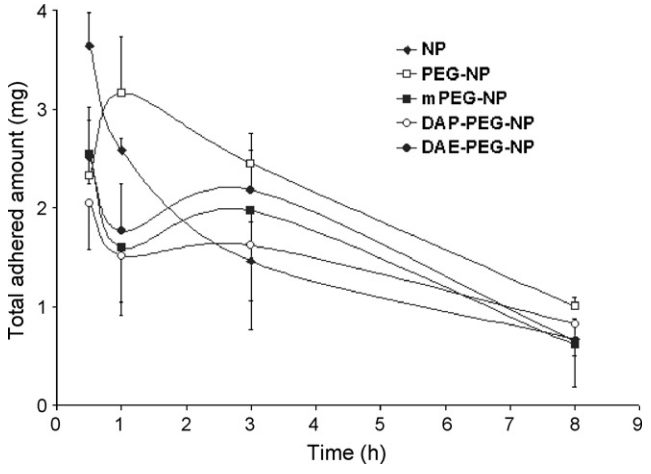

Fig. 4. Evolution of the adhered fraction of the nanoparticles within the whole gastrointestinal tract with the time after single oral dose (nanoparticle suspension of 10 mg/ml).

The specific distribution of the pegylated nanoparticles in the different parts of the gastrointestinal tract is illustrated in Fig. 5. Generally, all types of pegylated particles possessed higher affinity to adhere to intestinal than to the stomach mucosa. PEG-NP and mPEG-NP demonstrated homogenous distribution within the GIT during 8 h with a well-pronounced adhesion to the distal parts of small intestine. Like in the case of hydroxyl-PEGs, both amino-pegylated types of NP showed strong preference to the distal parts of small intestine. However, the distribution of DAE-PEG-NP was very similar to that of PEG-NP, whereas DAP-PEG-NP showed higher adhesion to caecum. Thus, the functional groups in the end of PEG-extended chains were not the most important reason for the different in vivo behaviour of nanoparticles. The different bioadhesive properties of DAP-PEG-NP were explained with the specific "loop" conformation of DAP-PEG on the nanoparticle surface.

Consequently, according to the surface modification of particles some conclusions could be made. The nanoparticles with a PEG-surface layer in a "brush" conformation (PEG-NP and DAE-PEG-NP) developed more intensive interactions with the mucosa than all the others. Eventual interaction between these nanoparticles and mucins could not be a reason for the high bioadhesion degree because mucin content and secretion diminishes in the distal parts of small intestine and is lower in the ileum (McQueen et al., 1983; Rubinstein and Tirosh, 1994). Probably, either an increasing hydrophilicity or protein repellent properties of PEG-layer enabled nanoparticle diffusion through mucus gel. This is in agreement with other studies where it was postulated that pegylated carriers penetrated easily through mucus layer (Vila et al., 2002; Huang et al., 2000). On the other hand, recently reported data showed that PEG-NP possessing surface "brush" layer developed less intensive interaction with mucin which further corresponded to better adhesion (Yoncheva et al., 2005a). In this view, the extended PEG-chains repelled mucin chains and would facilitate the proximal contact of PEG-NP with the cells of intestinal wall. On the contrary, the lower bioadhesive potential of mPEG-NP was due to the low presence of coating "brush" layer, whereas for DAP-PEG-NP to the fact that the double end coupled chains were not available for intensive interactions with the mucosa. Their higher adhesion to the caecum could be associated with the opening of the "loop" layer with the time, particularly after 3 h in the tract.

The parameters of the adhesion process were calculated according to the above data. As it could be seen in Table 3, the initial capacity of pegylated nanoparticles to develop bioadhesive forces was lower compared to the conventional NP. However, the area under the curve of bioadhesion (AUC_{adh}) for pegylated particles was higher suggesting an improvement in the intensity of the adhesion. This phenomenon was very well pronounced

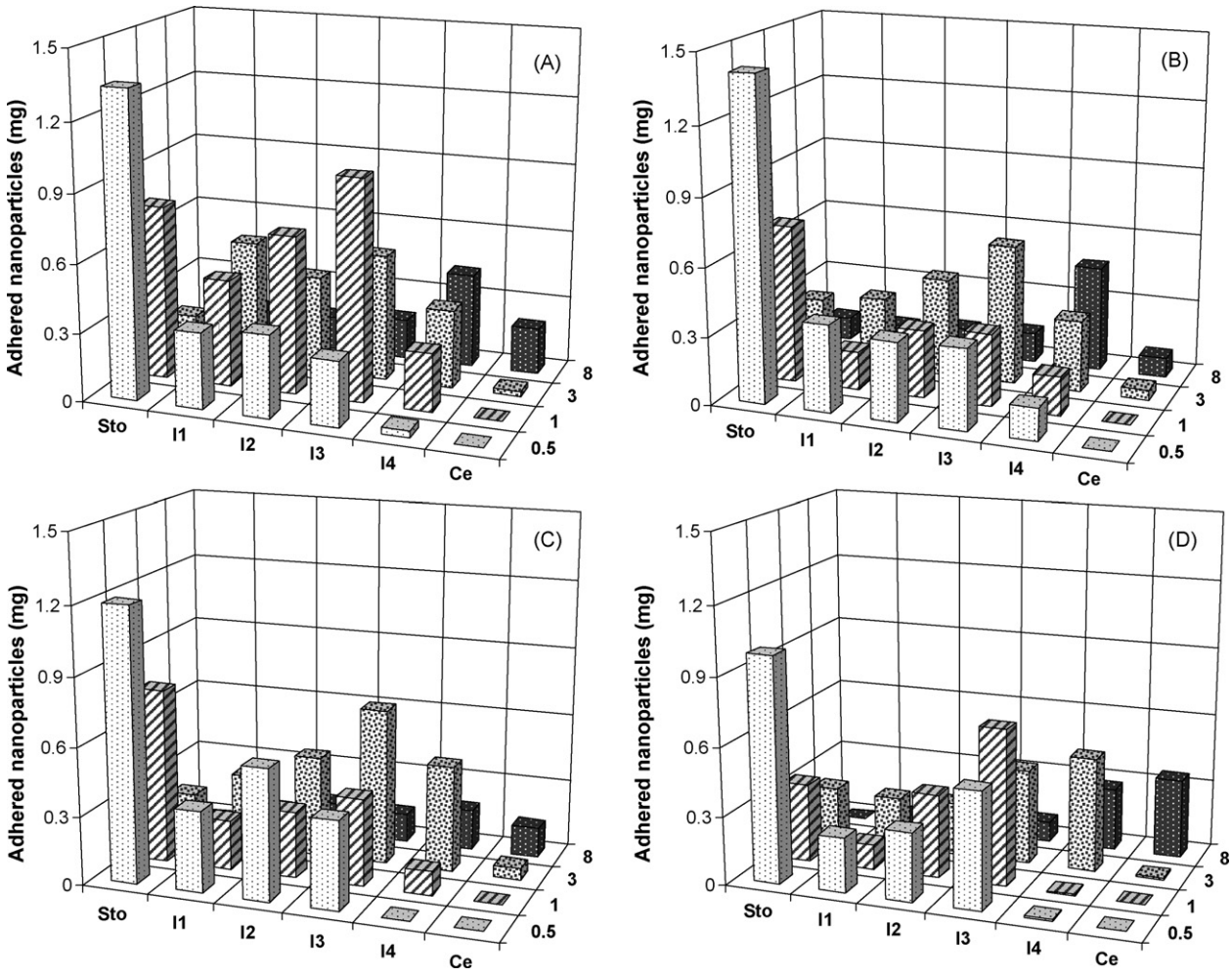

Fig. 5. In vivo distribution of the adhered fractions of nanoparticles in rat gastrointestinal tract after oral administration of aqueous nanoparticle suspension (10 mg/ml). Each value represents the mean of three experiments. (A) PEG-NP, (B) mPEG-NP, (C) DAE-PEG-NP and (D) DAP-PEG-NP. Plot: *x*-axis represents the adhered fraction (mg), *y*-axis illustrates the different gastrointestinal segments (Sto: stomach; I1, I2, I3, I4: parts of the small intestine; Ce: caecum) and *z*-axis marks the time of post-administration (h).

especially for PEG-NP, where 1.6-fold increase of AUC_{adh} was observed ($p < 0.01$ compared with NP). Based on these results some considerations could be made. The presence of "brush" layer seemed to increase the intensity of the adhesive phenomenon (AUC_{adh}). Particularly, the presence of OH-end groups on the surface (PEG-NP) appeared to be more effective than NH_2-end groups (DAE-PEG-NP) to induce the development of adhesive interactions. In addition, all pegylated nanoparticles demonstrated lower elimination rate (k_{adh}) and longer residence time (MRT_{adh}) compared to non-modified nanoparticles. A higher MRT implied a higher residence time of the adhered fraction to the mucosa. The longest residence possessed DAP-PEG-NP which lasted approximately 48.0 min more than non-modified NP. This fact could be explained with the different surface architecture of the particles as it was discussed above.

Table 3
Parameters of bioadhesion for the different types of pegylated nanoparticles

Nanoparticles	AUC_{adh} (mg h)	MRT (h)	k_{adh} (h^{-1})	$Q_{max.}$ (mg)
NP	11.83 ± 2.0	2.77	0.21 ± 0.01	3.64 ± 0.34
PEG-NP	16.19 ± 2.29**	3.11*	0.17 ± 0.01**	3.16 ± 0.57*
mPEG-NP	12.91 ± 6.84**	3.10*	0.16 ± 0.05**	2.55 ± 1.17*
DAE-PEG-NP	13.49 ± 1.76*	3.05*	0.17 ± 0.02**	2.51 ± 0.50**
DAP-PEG-NP	10.90 ± 5.04	3.57**	0.14 ± 0.10**	2.05 ± 0.47**

Data express mean ± S.D. ($n = 3$). Q_{max} (mg): maximal amount of nanoparticles adhered; AUC_{adh} (mg h): area under the curve of the adhered nanoparticles; k_{adh} (h^{-1}): terminal elimination rat of the adhered fraction; MRT_{adh} (h): mean residence time of the adhered fraction of the nanoparticles.

* $P < 0.05$; pegylated nanoparticles vs. control nanoparticles NP (Mann–Whitney *U*-test).

** $P < 0.01$; pegylated nanoparticles vs. control nanoparticles NP (Mann–Whitney *U*-test).

In general, it seemed that pegylation of nanoparticles might decrease their interaction with the lumen content (i.e. mucin). On the other hand, diffusion of the pegylated particles within the mucus layer would be facilitated. Thus, the nanoparticles could reach in an easier way the surface of the enterocytes, where they could develop adhesive interactions and, eventually, be "translocated".

3.3. Study on the nanoparticle transport.

Because of the better bioadhesive properties of PEG-NP they were selected as model particles for the transport study. The translocation of the pegylated nanoparticles was investigated by optical microscopy of isolated tissue segments after oral administration to rats. Another groups of animals received control solutions of FITC with concentration of 45 or 150 μg/ml, respectively. The first concentration represented the amount of FITC released from nanoparticles at the first hour of in vitro study (data not shown). The second solution possessed equivalent FITC-concentration as the amount of FITC loaded in PEG-NP (150 μg/mg). The micrographs of jejunal and ileal segments extracted from all animals demonstrated the presence of the marker into the enterocytes of intestinal villi. However, immunoreactivity for FITC when it was applied in the form of solutions showed less intensity than FITC-associated to PEG-NP (Fig. 6). This phenomenon was clearly observed with the increasing of the dilutions of FITC-antiserum added to the tissue samples. Here, the segments taken from nanoparticle treated rats still demonstrated high staining intensity in the enterocytes at 1:1000 dilution of the antiserum (Fig. 6C), whereas at the same dilution, the segments from the rats treated with FITC-solution showed almost absence of FITC into the cells (Fig. 6F). Based on these data it could be assumed that the higher amount of the marker visible in the epithelium of rats treated with

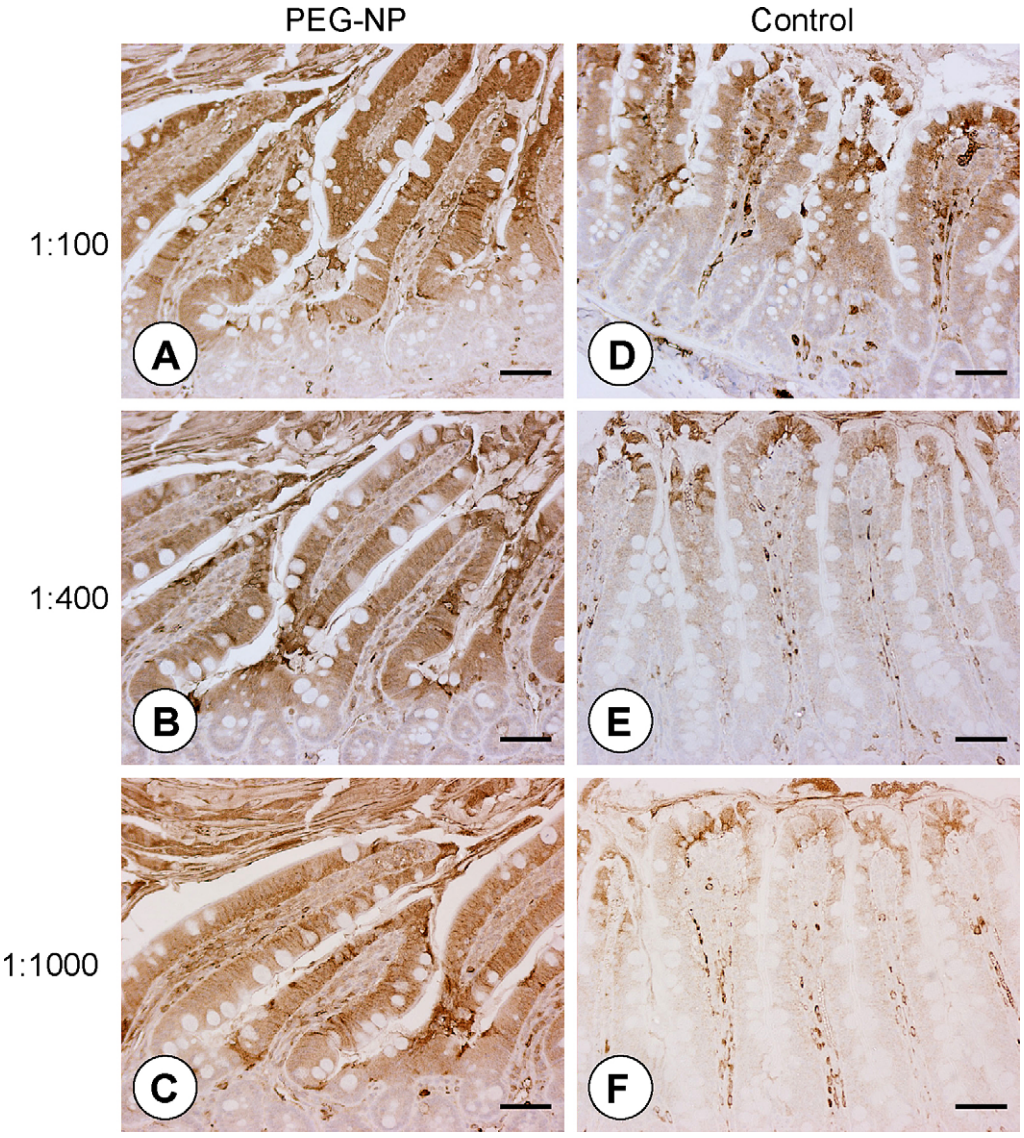

Fig. 6. Immunohistochemical staining of serial paraffin sections of rat ileum: rats receiving FITC-loaded PEG-NP (A–C) and rats treated with control FITC solution (150 μg/ml) (D–F). The decrease in immunostaining intensity with primary antibody dilution is more marked in control than in PEG-NP treated rats. Bars represent 30 μm.

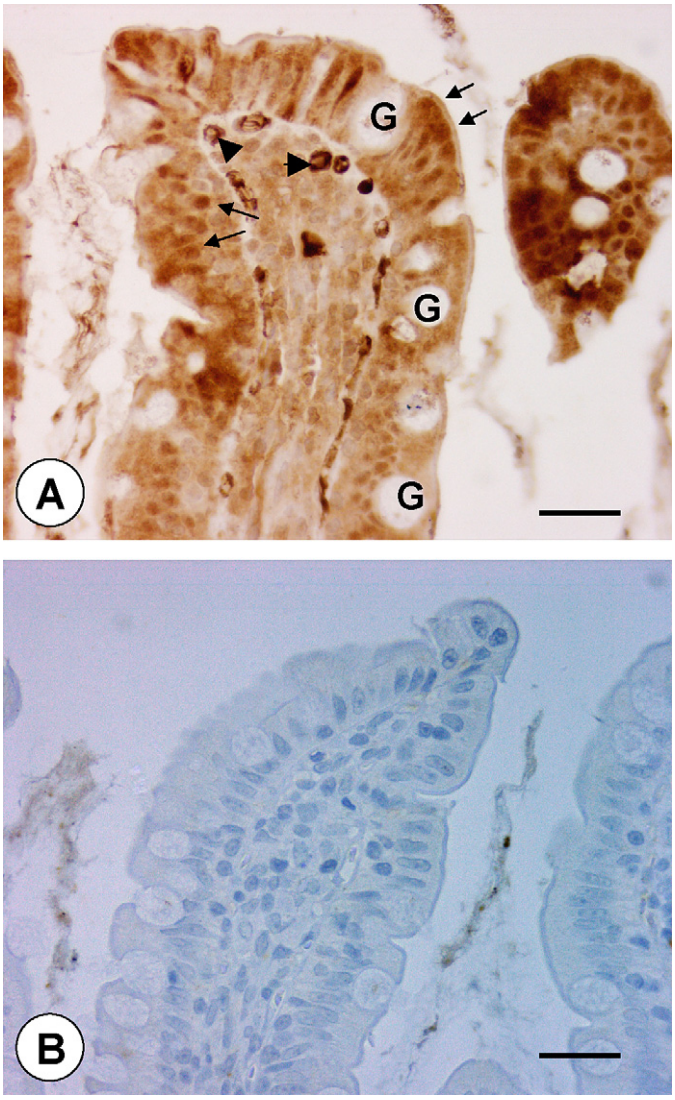

Fig. 7. Detail of intestinal villi: In rat receiving PEG-NP (A) immunoreactivity for FITC can be observed in the apical region of enterocytes (black arrows), enterocyte nuclei (white arrows) and capillaries (arrowheads); the goblet cells (marked with G) remain unstained. In negative controls no immunoreactivity was detected (B). Bars represent 20 μm.

PEG-NP was due to the transport of the FITC-associated PEG-NP. For comparison, the non-modified PVM/MA-nanoparticles were only able to cross partially the mucus layer and were not observed into the enterocytes (Yoncheva et al., 2005b). The results led us to suggest that PEG-NP interacted and bound directly with the cell surface rather than with the mucus components. In addition, the micrographs showed an absence of FITC-immunolabeling in the goblet cells (Fig. 7A). This fact could be considered like an indication that PEG-NP did not interact not only with the coating mucus but also with the mucus-secreting cells. Thus, the passage of PEG-NP occurred mainly through the absorptive enterocytes. These observations are in agreement with another study, where the authors reported that PEG-coating layer facilitated the transcellular transport of PECL-nanocapsules (De Campos et al., 2003). It is known, that after absorption particles could be included in cytoplasmic vesicles and discharged in the serosal spaces to gain access to the mesentheric lymph or blood. Here, the images also revealed an appearance of immunoreactivity for FITC into the blood capillaries of lamina propia suggesting further transport of PEG-NP across the epithelium. This fact corroborated a previous study dedicated on the transport of PEG-PLA-NP (loaded with radiolabeled tetanus toxoid) after oral administration (Tobio et al., 2000). The steady radioactivity levels observed between 6 and 24 h led to the conclusion that PEG-PLA-NP remained associated to the gastrointestinal mucosa, leading to a sustained drainage from the mucosa to the lymphatics and blood circulation. Another feature of the nanoparticle distribution was that some nuclei were found to be stained, thus, suggesting a penetration of FITC or FITC-NP through nuclear envelope (Fig. 7A). The latter could be of great interest, if PEG-NP were able to overcome the nuclear membrane, this would be crucial for improving the performance of gene-delivery. So, the exact mechanism of the interaction between pegylated nanoparticles and enterocytes and their subsequent distribution should be investigated. Electrostatic interactions between negatively charged glycocalyx on the enterocyte surface and PEG-chains extended from the nanoparticles were excluded because of the negative charge of the latter themselves. Some studies demonstrated that hydrophobic type of interactions could be established between cell membrane and polystyrene nanoparticles known as very hydrophobic (Hillery and Florence, 1996). Here, hydrophobic interactions probably did not occur because the hydrophilicity of the surface PEG-layer could be considered as obstacle. In all cases, more experiments would be needed in order to detail the mechanism of the translocation of the pegylated nanoparticles through intestinal mucosa.

4. Conclusions

The different type of surface architecture of the pegylated nanoparticles developed here influenced their bioadhesive properties. In general, all types of pegylated particles possessed higher affinity to adhere to intestinal rather than to the stomach mucosa. Higher bioadhesive potential was observed in the case of PEG-NP and DAE-PEG-NP which was attributed to the flexibility and specific properties of the surface "brush" layer of these particles. Further, microscopic observations showed an intracellular transport of PEG-NP with preferable location in the apical area of enterocytes.

Acknowledgements

This work was supported by "Ministerio de Ciencia y Tecnología" (Projects SAF2001-0690-C03 and AGL2004-07088-C03-02), and Instituto de Salud Carlos III (Grant RITC Cancer C1/03), Fundación Roviralta and Fundación Universitaria de Navarra in Spain.

References

Arbos, P., Arangoa, M.A., Campanero, M.A., Irache, J.M., 2002. Quantification of the bioadhesive properties of protein-coated PVM/MA nanoparticles. Int. J. Pharm. 242, 129–136.

Arbos, P., Campanero, M.A., Arangoa, M.A., Renedo, M.J., Irache, J.M., 2003. Influence of the surface characteristics of PVM/MA nanoparticles on their bioadhesive properties. J. Control. Rel. 89, 19–30.

De Ascentiis, A., DeGrazia, J.L., Bowman, C.N., Colombo, P., Peppas, N.A., 1995. Mucoadhesion of poly(2-hydroxyethyl methacrylate) is improved when linear poly(ethylene oxide) chains are added to the polymer network. J. Control. Rel. 33, 197–201.

De Campos, A.M., Sanchez, A., Gref, R., Calvo, P., Alonso, M.J., 2003. The effect of a PEG versus a chitosan coating on the interaction of drug colloidal carriers with the ocular mucosa. Eur. J. Pharm. Sci. 20, 73–81.

Florence, A.T., 1997. The oral absorption of micro- and nanoparticulate: neither exceptional nor unusual. Pharm. Res. 14, 259–266.

Hillery, A.M., Florence, A.T., 1996. The effect of absorbed poloxamer 188 and 407 surfactants on the intestinal uptake of 60 nm polystyrene particles after oral administration in the rats. Int. J. Pharm. 132, 123–130.

Hodges, G.M., Carr, E.Q., Hazzard, R.A., O'Reilly, C., Carr, K., 1995. A commentary on morphological and quantitative aspects of microparticle translocation across the gastrointestinal mucosa. J. Drug Target. 3, 57–60.

Huang, Y., Leobandung, W., Foss, A., Peppas, N., 2000. Molecular aspects of muco- and bioadhesion: tethered structures and site-specific surfaces. J. Control. Rel. 65, 63–71.

Hussain, N., Jani, P.U., Florence, A.T., 1997. Enhanced oral uptake of tomato lectin-conjugated nanoparticles in the rat. Pharm. Res. 14, 613–618.

Irache, J.M., Durrer, D., Duchene, D., Ponchel, G., 1996. Bioadhesion of lectin-latex conjugates to rat intestinal mucosa. Pharm. Res. 13, 1716–1719.

Isosaki, K., Seno, N., Matsumoto, I., Koyama, T., Moriguchi, S., 1992. Immobilization of protein ligands with methyl vinyl ether-maleic anhydride copolymer. J. Chromatogr. 597, 123–128.

Iwanaga, K., Ono, S., Narioka, K., Morimoto, K., Kakemi, M., Yamashita, S., Nango, M., Oku, N., 1997. Oral delivery of insulin by using surface coating liposomes. Improvement of stability of insulin in GIT. Int. J. Pharm. 157, 73–80.

Kawashima, Y., Yamamoto, H., Takeuchi, H., Kuno, Y., 2000. Mucoadhesive DL-lactide/glycolide copolymer nanospheres coated with chitosan to improve oral delivery of elcatonin. Pharm. Dev. Technol. 5, 77–85.

Kreuter, J., 1991. Peroral administration of nanoparticles. Adv. Drug Del. Rev. 7, 71–86.

Le Ray, A.M., Vert, M., Gautier, J.C., Benoit, J.P., 1994. Fate of [^{14}C] poly(DL-lactide-*co*-glycolide) nanoparticles after intravenous and oral administration to mice. Int. J. Pharm. 106, 201–211.

McQueen, S., Hutton, D., Allen, A., Garner, A., 1983. Gastric and duodenal surface mucus gel thickness in rat: effects of prostaglandins and damaging agents. Am. J. Physiol. 245, G388–G393.

Otsuka, H., Nagasaki, Y., Kataoka, K., 2003. PEGylated nanoparticles for biological and pharmaceutical applications. Adv. Drug Del. Rev. 55, 403–419.

Peracchia, M.T., Vauthier, C., Puisieux, F., Couvreur, P., 1997. Development of sterically stabilized poly(isobutyl 2-cyanoacrylate) nanoparticles by chemical coupling of poly(ethylene glycol). J. Biomed. Mater. Res. 34, 317–326.

Pompe, T., Zschoche, S., Herold, N., Salchert, K., Gouzy, M.F., Sperling, C., Werner, C., 2003. Maleic anhydride copolymers—a versatile platform for molecular biosurface engineering. Biomacromolecules 4, 1072–1079.

Rubinstein, A., Tirosh, B., 1994. Mucus gel thickness and turnover in the gastrointestinal tract of the rat, responses to cholinergic stimulus and implication for mucoadhesion. Pharm. Res. 11, 794–799.

Ropert, C., Bazile, D., Brendenbach, J., Marlard, M., Veillard, M., Spenlehauer, G., 1993. Fate of C radiolabeled poly(DL-lactic acid) nanoparticles following oral administration to rats. Colloid. Surf. B: Biointerf. 1, 233–239.

Sakuma, S., Sudo, R., Suzuki, N., Kikuchi, H., Akashi, M., Hayashi, M., 1999. Mucoadhesion of polystyrene nanoparticles having surface hydrophilic polymeric chains in the gastrointestinal tract. Int. J. Pharm. 177, 161–172.

Schmidt, U., Zschoche, S., Werner, C., 2003. Modification of poly(octadecene-alt-maleic anhydride) films by reaction with functional amines. J. Appl. Polym. Sci. 87, 1255–1266.

Takeuchi, H., Yamamoto, H., Niwa, T., Hino, T., Kawashima, Y., 1996. Enteral absorption of insulin in rats from mucoadhesive chitosan-coated liposomes. Pharm. Res. 13, 896–901.

Tobio, M., Sanchez, A., Vila, A., Soriano, I., Evora, C., Vila-Jato, J.L., Alonso, M.J., 2000. The role of PEG on the stability in digestive fluids and in vivo fate of PEG-PLA nanoparticles following oral administration. Colloid Surf. B: Biointerf. 18, 315–323.

Vila, A., Sanchez, A., Tobio, M., Calvo, P., Alonso, M.J., 2002. Design of biodegradable particles for protein delivery. J. Control. Rel. 78, 15–24.

Yoncheva, K., Lizarraga, E., Irache, J.M., 2005a. Pegylated nanoparticles based on poly(methyl vinyl ether-*co*-maleic anhydride): preparation and evaluation of their bioadhesive properties. Eur. J. Pharm. Sci. 24, 411–419.

Yoncheva, K., Gomez, S., Campanero, M.A., Gamazo, C., Irache, J.M., 2005b. Bioadhesive properties of pegylated nanoparticles. Exp. Opin. Drug Deliv. 2, 205–218.